AGU PUBLICATIONS

Geophysical Research Letters

RESEARCH LETTER
10.1002/2014GL063004

Key Points:
- A novel morphodynamic model describes field-observed onshore sandbar migration
- Both wave velocity and acceleration skewness are equally important
- Accelerations control the inner surf zone; velocities dominate the shoaling zone

Supporting Information:
- Readme
- Text S1
- Text S2
- Text S3
- Data Set S1
- Data Set S2
- Data Set S3
- Data Set S4
- Data Set S5
- Data Set S6
- Data Set S7
- Data Set S8
- Data Set S9
- Data Set S10
- Data Set S11
- Data Set S12
- Data Set S13
- Data Set S14
- Data Set S15
- Data Set S16
- Data Set S17
- Data Set S18
- Data Set S19
- Data Set S20
- Data Set S21
- Data Set S22

Correspondence to:
A. Fernández-Mora,
m.fernandezmora@utwente.nl

Citation:
Fernández-Mora, A., D. Calvete, A. Falqués, and H. E. de Swart (2015), Onshore sandbar migration in the surf zone: New insights into the wave-induced sediment transport mechanisms, *Geophys. Res. Lett.*, *42*, 2869–2877, doi:10.1002/2014GL063004.

Received 7 JAN 2015
Accepted 5 MAR 2015
Accepted article online 10 MAR 2015
Published online 17 APR 2015

Onshore sandbar migration in the surf zone: New insights into the wave-induced sediment transport mechanisms

A. Fernández-Mora[1], D. Calvete[1], A. Falqués[1], and H. E. de Swart[2]

[1]Department of Applied Physics, Universitat Politècnica de Catalunya·BarcelonaTech, Barcelona, Spain, [2]Institute for Marine and Atmospheric Research, Utrecht University, Utrecht, Netherlands

Abstract We present a novel process-based morphodynamic model, which includes transport processes due to both velocity and acceleration skewness and a new formulation for intrawave motions, that successfully simulates observations of onshore sandbar migration. Results confirm findings of previous studies, in which each process was considered separately and in which sediment transport was computed from the observed water motion. However, our results indicate that accounting for the joint action of both velocity and acceleration skewnesses causes major improvement of the modeled onshore bar migration and is essential to accurately model the evolution of the entire cross-shore bottom profile, when compared with observations. We also demonstrate that the morphodynamics in the shoaling zone are dominated by velocity skewness (bed shear stresses), while sediment transport induced by acceleration skewness (pressure gradients) controls the morphodynamics in the inner surf zone.

1. Introduction

Surf zone sandbars are of primary importance for the persistence of sandy shores, as they protect the beach during storms causing wave dissipation through wave breaking. They also constitute a reservoir for the exchange of sand between the submerged and the dry beach. Since the morphology of sandbars and the surf zone hydrodynamics are intrinsically coupled, understanding sandbar dynamics is important for coastal protection, human activities (e.g., industry, tourism, and surfing), or environmental issues (water quality, pollutant dispersion, biologic activity, etc). Sandbar morphodynamics has a strong three-dimensional nature which is linked to wave breaking, inducing horizontal circulation in the surf zone (longshore current and rip currents). Despite the 3-D nature of nearshore morphodynamics, in many cases sandbars are remarkably longshore uniform and it is assumed that cross-shore, rather than longshore processes, control the formation and migration of bars.

There is general consensus with regard to the underlying mechanisms causing the offshore migration of sandbars: during storms, strong waves drive near-bottom intense offshore directed flow (undertow) that moves bars offshore [*Short*, 1999]. In contrast, the mechanics of onshore sandbar migration is still a controversial topic. Under low energetic conditions, currents are weak, and sediment transport is driven mostly by near-bottom wave orbital motion. However, early attempts to simulate onshore sandbar migration using wave-averaged sediment transport parameterizations based on bottom stresses (e.g., Meyer-Peter and Müller power law) were not successful [*Roelvink and Stive*, 1989; *Wright et al.*, 1991; *Thornton and Humiston*, 1996; *Rakha et al.*, 1997; *Gallagher et al.*, 1998]. It was argued by *Elgar et al.* [2001] that this discrepancy was due to the sediment transport formulation, which considers velocity skewness but no acceleration skewness (skewness is here defined as the wave averaging of the third power of a variable). This was confirmed by *Hoefel and Elgar* [2003], who used a bed load sediment transport proxy based on the acceleration skewness developed by *Drake and Calantoni* [2001] to successfully model an observed onshore sandbar migration event during the Duck94 experiment at the Field Research Facility-USACE Army at Duck, North Carolina, USA. The contribution of *Hoefel and Elgar* [2003] suggested that acceleration skewness was indispensable to correctly model onshore bar migration.

Interestingly, *Hsu et al.* [2006] were also able to model onshore migration for the same event using a modified energetic-based sediment transport model that distinguishes the action of the wave stirring in sediment transport from the action of waves plus currents. As a result, it is unclear which mechanism, velocity or acceleration skewness, is the main driver of onshore sandbar migration. *Hoefel and Elgar* [2003] and *Hsu et al.* [2006] obtained their results by calculating the sediment transport from measured

near-bottom velocities (3 h averaged) of current meters at 40–100 cm from the bottom during the Duck94 experiment. These models use the hydrodynamic measurements taken on the real bathymetry to compute bottom changes. As real and computed bathymetry may diverge, these models do not address the morphodynamic coupling and thus lack on the forecasting abilities of fully process-based morphodynamical models.

Such process-based models are nowadays available, and they include a detailed description of the intrawave motion. In the framework of wave-averaged and depth-integrated models, a parameterization that accurately describes that motion is a key factor. *Ruessink et al.* [2012] used an adjusted version of the parameterization for orbital motion of *Abreu et al.* [2010] to compute the morphological change of a cross-shore profile by using the CROSMOR model [*Van Rijn*, 2007a, 2007b] for a 5 day simulation under steady wave forcing. They succeeded to model onshore sandbar migration patterns, and, in this sense, their results encourage the use of this approximation as a plausible way to include wave skewness and asymmetry effects on sediment transport computation in beach evolution models. *Van der Werf et al.* [2012], using the *Ruessink et al.* [2012] parameterization, tested a total load transport formula against experimental data [*Roelvink and Reniers*, 1995; *Grasso et al.*, 2011]. In this line, *Fernandez-Mora et al.* [2013] considered the extended energetic model of *Hsu et al.* [2006] and the intrawave parameterization of *Ruessink et al.* [2012] to model bar migrations during 72 days at Duck, North Carolina, USA. Similarly, *Dubarbier et al.* [2013], also by using the approach for the intrawave motion, combined the transport of *Hoefel and Elgar* [2003] and *Hsu et al.* [2006] to model the observed migration of a bar in a flume.

However, those papers did not examine the joint action of both wave velocity and wave acceleration skewness comparing the role of each one on onshore sandbar migration mechanism. Consequently, in this study a morphodynamic process-based model is used that accounts for the intrawave orbital velocity approximation of *Ruessink et al.* [2012] and includes the two main drivers of sediment transport, i.e., velocity skewness and acceleration skewness. A third sediment transport formulation that combines those sediment transport formulas is presented as well. Following the research of *Hoefel and Elgar* [2003] and *Hsu et al.* [2006], the process-based model is used to model the onshore migration event of Duck94. The three sediment transport models are calibrated separately to obtain the best fit for this event. A comparison of the results of the three transports is done for two main purposes. The first is to confirm the results of *Hoefel and Elgar* [2003] and *Hsu et al.* [2006] with a process-based model. That is, sediment transport formulations based on either velocity skewness or on acceleration skewness can reproduce the onshore sandbar migration, and, therefore, both processes may act in nature with similar effects. The second purpose is to elucidate which is the role of velocity skewness and acceleration skewness in the mechanism of onshore sandbar migration. The model will be introduced in the next section. Afterward, numerical results and a discussion will be presented, followed by the conclusions.

2. Numerical Model and Setup

2.1. Model

The process-based model considers depth- and wave-averaged momentum and mass balance equations coupled with wave- and roller-energy conservation, Snell's law, and the dispersion relationship (see *Fernandez-Mora et al.* [2013] for detailed information). The formulation of *Ruessink et al.* [2012], adapted from *Abreu et al.* [2010], is used to model the intrawave near-bottom velocity, that is, the function of the root-mean-square wave height H, the wave period T, and the depth D. Time- and depth-averaged undertow is computed from mass transport due to wave and surface rollers. A detailed description of the model formulation is given in the supporting information.

The bottom evolution is governed by the sediment mass conservation equation, which in the present context (longshore uniformity) reads

$$(1-n)\frac{\partial z_b}{\partial t}+\frac{\partial Q_x}{\partial x}=0 \tag{1}$$

Here z_b is the bed level, t is time, n is the porosity of sediment (set to 0.4), and Q_x is the wave-averaged sediment transport in the cross-shore direction. The x axis points in the seaward direction.

To determine which is the governing mechanism driving onshore sandbar migration process, sediment transport is computed considering two transport formulas, one related to velocity skewness [*Hsu et al.*, 2006] and the other one related to acceleration skewness [*Hoefel and Elgar*, 2003].

2.1.1. The Velocity Skewness Transport

The velocity skewness transport (hereinafter SkV transport) follows the sediment transport description given by *Hsu et al.* [2006] complemented with a diffusive transport term Q_D. It is defined as

$$Q_{\mathrm{SkV}} = Q_V + Q_C + Q_D \tag{2}$$

in which Q_V and Q_C are the net sediment transport due to waves and currents given by *Hsu et al.* [2006], respectively:

$$Q_V = \frac{C_w}{(s-1)g}\left(\frac{\varepsilon_B}{\tan\varphi}\langle|\vec{U}_0|^2 U_{0,x}\rangle + \frac{\varepsilon_S}{W_0}\langle|\vec{U}_0|^3 U_{0,x}\rangle\right) \tag{3}$$

$$Q_C = \frac{C_c}{(s-1)g}\left(\frac{\varepsilon_B}{\tan\varphi}\langle|\vec{U}_t|^2\rangle U_x + \frac{\varepsilon_S}{W_0}\langle|\vec{U}_t|^3\rangle U_x\right) \tag{4}$$

Here s is the specific gravity (set to 2.65), g is the acceleration due to gravity, φ is the friction angle ($\tan\varphi = 0.63$), ε_B and ε_S are transport efficiency factors (set to $\varepsilon_B = 0.135$ and $\varepsilon_S = 0.015$ [*Thornton and Humiston*, 1996; *Gallagher et al.*, 1998]), W_0 is the sediment fall velocity, $\vec{U}_0$ is the wave orbital velocity vector, $\vec{U}_t$ is the total velocity vector (waves plus currents), and $\vec{U}$ is the current velocity vector, related to the longshore current and the offshore-directed undertow velocity. Subscript x indicates the cross-shore component. Vertical bars indicate the magnitude of the vector and the angular brackets <> the time averaging of the vector. Note that these sediment transport terms neglect settling lag effects, and thus, the transport related to the Stokes drift is not considered, as was done in *Henderson et al.* [2004]. Values of the waves and currents friction coefficients C_w and C_c will be calibrated by fitting the SkV transport model results with observations, to verify that a sediment transport formula based on velocity skewness can explain the onshore migration of the bar.

The term Q_D in equation (2) represents a diffusive transport resulting from the tendency of sand to move downslope:

$$Q_D = \lambda_d\, \nu(x)\left(\frac{1}{\tan\varphi - \mathrm{d}z_b/\mathrm{d}x}\right)\left(\frac{\mathrm{d}z_b/\mathrm{d}x}{\tan\varphi}\right) \tag{5}$$

where $\mathrm{d}z_b/\mathrm{d}x$ is the bottom slope, λ_d is a coefficient to be set in the calibration, together with the friction coefficients C_w and C_c, and ν is a term that is specified in the supporting information.

2.1.2. The Acceleration Skewness Transport

The acceleration skewness transport model (hereinafter SkA transport) is based on the model of *Hoefel and Elgar* [2003], complemented with the transport due to mean currents (Q_C) and the diffusive transport (Q_D) as are given in equations (4) and (5), respectively, to provide a more accurate description of the physics involving sediment transport processes. The SkA transport reads

$$Q_{\mathrm{SkA}} = Q_A + Q_C + Q_D \tag{6}$$

Here Q_A is the acceleration-driven transport given by *Hoefel and Elgar* [2003]:

$$Q_A = \begin{cases} K_a(a_{\mathrm{spike},x} - \mathrm{sign}(a_{\mathrm{spike},x})a_{\mathrm{cr}}) & a_{\mathrm{spike},x} \geq a_{\mathrm{cr}} \\ 0 & a_{\mathrm{spike},x} < a_{\mathrm{cr}} \end{cases} \tag{7}$$

in which K_a is a constant ($m\,s$), a_{cr} is the threshold acceleration (set to 0.5 ms^{-2}), and $a_{\mathrm{spike}} = \langle a(t)^3\rangle / \langle a(t)^2\rangle$, which is related to the acceleration skewness [*Drake and Calantoni*, 2001]. Although the original expression of the *Hoefel and Elgar* [2003] formula accounted just for the bed load contribution, in the present work it is assumed that the K_a constant accounts for the contribution of both bed load and suspended load. Subscript x indicates the cross-shore component. The acceleration $\vec{a}(t)$ is computed as the local time derivative of the total velocity $\vec{U}_t$. Similarly as for the SkV transport, K_a, C_c, and λ_d are parameters to be calibrated by fitting results of the SkA transport model with observations, in order to address that acceleration skewness can explain the onshore migration.

2.1.3. The Combined Transport

In order to account for all previous transport terms, a new sediment transport formulation is considered that combines the SkV and the SkA transport formulas and therefore contains the terms Q_V, Q_A, Q_C, and Q_D of equations (3)–(5) and (7). To systematically analyze the relative importance of the velocity skewness and the acceleration skewness on onshore sandbar migration, the new sediment transport model (hereinafter MiX transport) is defined in terms of the SkV and the SkA transports as follows:

$$Q_{\mathrm{MiX}} = \alpha_V Q_V^{\mathrm{SkV}} + \alpha_A Q_A^{\mathrm{SkA}} + \beta \left[\alpha_V Q_C^{\mathrm{SkV}} + \alpha_A Q_C^{\mathrm{SkA}}\right] + \gamma \left[\alpha_V Q_D^{\mathrm{SkV}} + \alpha_A Q_D^{\mathrm{SkA}}\right] \tag{8}$$

In the expression above, the superscripts SkV and SkA denote, respectively, the sediment transport terms from the SkV and the SkA models once they have been calibrated separately. The coefficients α_V, α_A, β, and γ are four independent coefficients that weight the different transport terms. The coefficients α_V and α_A weight the amount of the action of velocity skewness and acceleration skewness on the MiX transport, in such a way that the set $[\alpha_V, \alpha_a, \beta, \gamma] = [1, 0, 1, 1]$ is the calibrated SkV transport, and the set $[\alpha_V, \alpha_a, \beta, \gamma] = [0, 1, 1, 1]$ leads to the calibrated SkA transport. The optimum values of the four coefficients $[\alpha_V, \alpha_A, \beta, \gamma]$ will result from a calibration with observed onshore sandbar migration.

2.2. Data, Experimental Setup, and Calibration

The test period concerns the onshore sandbar migration event during the Duck94 field experiment at the Field Research Facility (FRF) at Duck, NC [*Gallagher et al.*, 1998; *Elgar et al.*, 2001]. This sequence is characterized by a 30 m onshore migration of the sandbar under relatively low energy wave conditions from 21 to 28 September 1994. The hydrodynamics of the model are initialized with the cross-shore profile bathymetry of 21 September and are driven with the wave data sampled by the 8 m water depth, 925 m offshore FRF pressure gauges that supply the RMS wave heights, period and direction each 3 h during the Duck94 experiment, and the water level is given by the NOAA pressure gauge at the end of the FRF pier (sampled each 6 min).

The hydrodynamics and the morphological change are computed every 300 s over a nonuniform grid. Sand grain diameter is considered constant along the profile and set to $d_{50} = 0.2$ mm with the corresponding settling velocity $W_0 = 0.025$ ms^{-1} [*Hsu et al.*, 2006]. Hydrodynamics parameters are set according to previous calibrations [*Fernandez-Mora et al.*, 2013], using the wave height, setup, and longshore currents data along 10 cross-shore profiles and 39 wave conditions during the SandyDuck'97 experiment at the FRF-Duck, NC.

The model skill is quantified through a "Brier skill score" type parameter [*Van Rijn et al.*, 2003; *Ruessink*, 2005] defined as

$$S = 1 - \frac{\int_{x_1}^{x_2} (z_b(x) - z_{b,\mathrm{obs}}(x))^2 \mathrm{d}x}{\int_{x_1}^{x_2} (z_{b,\mathrm{obs}}(x) - z_{b0,\mathrm{obs}}(x))^2 \mathrm{d}x} \tag{9}$$

where $z_b(x)$ is the bottom elevation computed by the model at the end of the event (28 September 1994), $z_{b,\mathrm{obs}}(x)$ is the observed bottom elevation at that date, $z_{b0,\mathrm{obs}}(x)$ is the observed elevation at the beginning of the event (21 September 1994) along the cross-shore direction x, and x_1 and x_2 limit the cross-shore profile zone where the skill is computed. The values of the skill S range within $[-\infty < S \leq 1]$. Perfect agreement between results and observations is given by an $S = 1.0$. Values $0 < S < 1$ correspond to better simulations than assuming no bottom change ($S = 0$).

As the aim of the present work is focused on sandbar morphodynamics, the skill S is considered along the bar zone $S_{\mathrm{bar}} = S(185\ \mathrm{m}, 265\ \mathrm{m})$. In addition, the S related to the inner zone $S_{\mathrm{in}} = S(155\ \mathrm{m}, 185\ \mathrm{m})$, the offshore zone $S_{\mathrm{off}} = S(265\ \mathrm{m}, 335\ \mathrm{m})$, and the entire profile $S_{\mathrm{tot}} = S(155\ \mathrm{m}, 335\ \mathrm{m})$ will be considered as well.

The SkV and SkA transports are calibrated to maximize the skill S_{bar} for the Duck94 onshore sandbar migration event. The sediment transport parameters are considered in the following ranges: the waves and currents friction coefficients C_w and C_c from 0 to 5×10^{-3}, the K_a constant from 0 to 1×10^{-3} m s, and the coefficient λ_d from 0 to 1×10^{-2}. The set of parameters achieving the global maximum value of S_{bar} are considered the best fitting parameters for the SkV and SkA transport models. Using these parameters, the MiX transport is calibrated ranging the weighting parameters α_V, α_A, β, and γ from 0 to 1.50 to get the maximum value of S_{bar}.

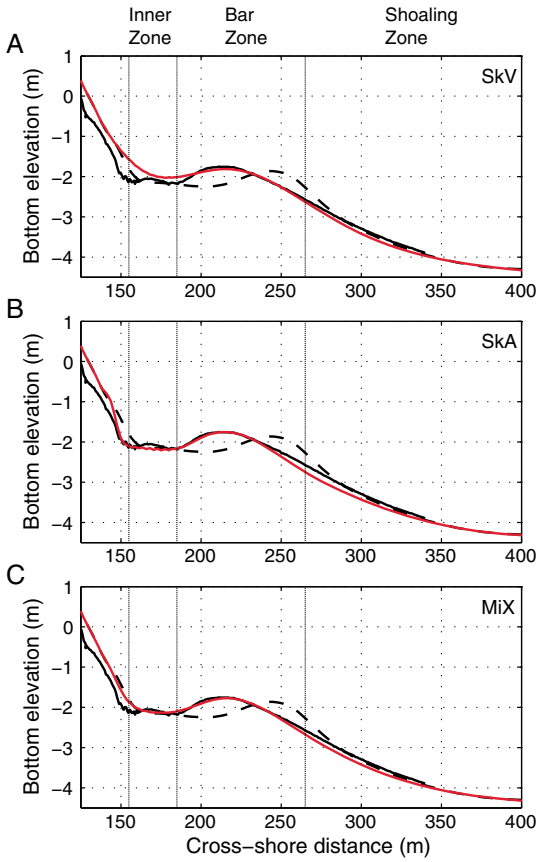

Figure 1. Morphological evolution (red line) of the Duck94 onshore migration event for (a) the SkV transport, (b) the SkA transport, and (c) the MiX transport. The initial measured profile (21 September, black dashed line) and final measured profile (28 September, black solid line) are shown in each panel.

3. Results and Discussion

With the best fits for the SkV transport ($C_w = 3.9\times10^{-4}$, $C_c = 1.0\times10^{-5}$, $\lambda_d = 3.0\times10^{-3}$) and for the SkA transport ($K_a = 1.4 \times 10^{-5}$ m s, $C_c = 1.4 \times 10^{-4}$, $\lambda_d = 4.2 \times 10^{-4}$) , both bar crest position and growth are properly reproduced (see Figures 1a and 1b). In terms of the skill of each model, the result for the SkV transport is slightly more accurate than the one obtained with the SkA transport ($S_{\text{bar}}^{\text{SkV}} = 0.965$ and $S_{\text{bar}}^{\text{SkA}} = 0.955$). This yields to our first and second key results: the process-based model (i) confirms the findings of *Hoefel and Elgar* [2003] and *Hsu et al.* [2006] and (ii) supports the considerations of *Hsu et al.* [2006] that indeed both sediment transport mechanisms can yield the onshore bar migration.

Note that each transport mechanism leads to different behavior outside the sandbar zone. The SkA transport performs quite better in the inner region, reproducing the nearshore erosion, but overestimates the erosion on the bar seaward face. On the contrary, the SkV performs better in the outer region, although it is not able to simulate the nearshore erosion and the trough shape. These behaviors have been quantified (see Table 1) by the skill in the inner surf zone (S_{in}), the shoaling zone (S_{out}), and the entire profile (S_{tot}). Beach profile evolution for the Duck94 onshore event is also computed using the MiX transport.

Considering the best fits for the MiX transport, the model reproduces accurately the crest position and depth of the sandbar and trough shape (Figure 1c). The best fit is given by $\alpha_V = 0.45$ and $\alpha_A = 0.45$ and has a maximum skill of $S_{\text{bar}}^{\text{MiX}} = 0.981$, larger than the SkV and the SkA skill values. Furthermore, when the rest of the profile is considered (see S_{in}, S_{out}, and S_{tot} in Table 1), the MiX transport achieves the overall best performance. The bed changes due to the MiX transport captures the best trends of the ones related to the SkA and the SkV transports, collecting both behaviors on modeling the inner surf zone and shoaling zone shapes (see Figure 1c). In this sense, their joint action is essential to model accurately the evolution of the entire profile during this onshore sandbar migration event.

This is further evidenced by analyzing the contribution of each term of the MiX transport in the bottom change (see Figure 2). At the Duck94 onshore sandbar migration event, the bottom evolution modeled

Table 1. Summary of the Maximum Model Skill S and the Corresponding $[\alpha_V, \alpha_A, \beta, \gamma]$ Parameters at the Bar, Inner and Offshore Zones, and the Total Profile for the SkV, SkA, and MiX Transport[a]

	Bar	Inner Zone	Offshore Zone	Full Profile				
	S_{bar}	S_{in}	S_{off}	S_{tot}				
(x_1, x_2)	(185, 265)	(155, 185)	(265, 335)	(155, 335)	α_V	α_A	β	γ
SkV	0.965	0.623	**0.876**	0.604	1.00	0.00	1.00	1.00
SkA	0.955	**0.927**	0.742	0.744	0.00	1.00	1.00	1.00
MiX	**0.981**	0.893	0.851	**0.816**	0.45	0.45	0.40	1.00

[a]Values in bold corresponds to the best Model Skill at each part of the profile.

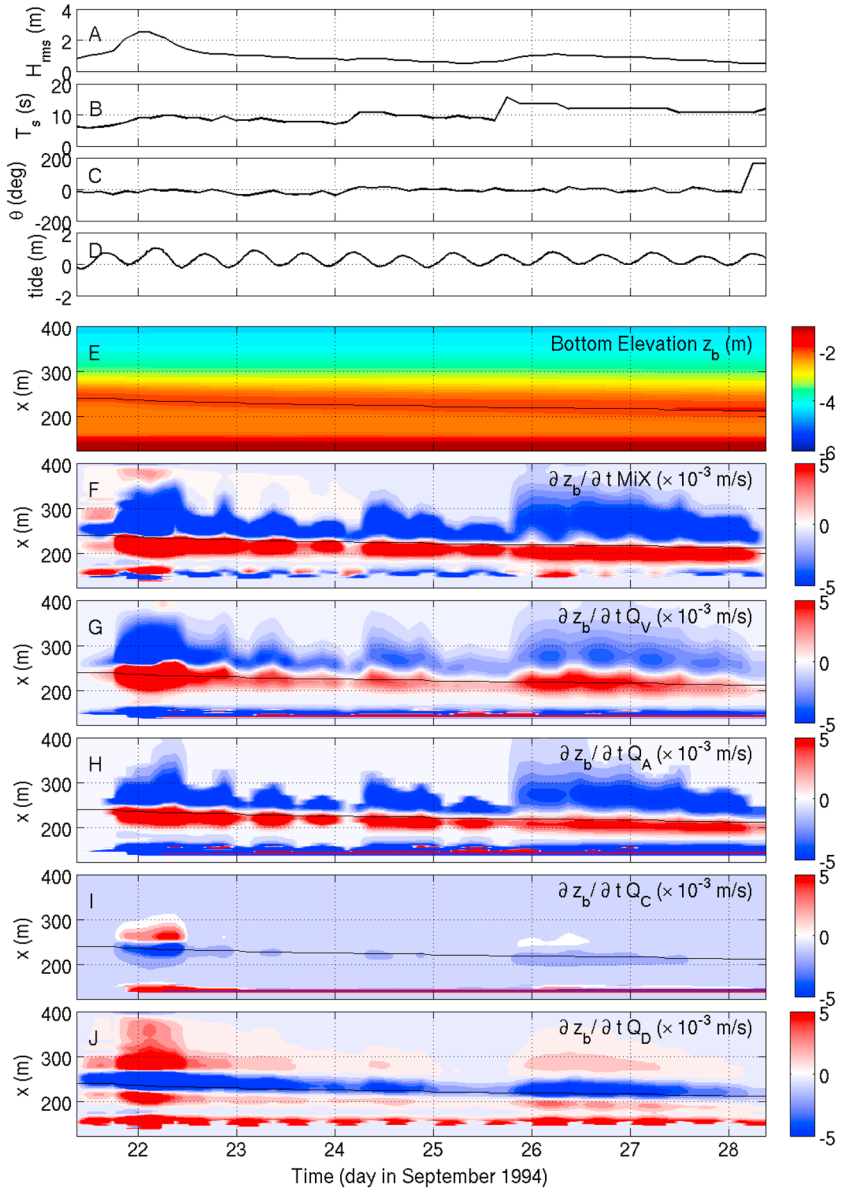

Figure 2. Time series of the (a) observed offshore wave height H_{rms}, (b) period T_p, (c) angle of incidence θ, and (d) tide level. (e) Bottom evolution z_b during the Duck94 experiment for the MiX transport; (f) bottom changes driven by the MiX transport; and bottom changes driven by each terms of the MiX transport: (g) Q_V, (h) Q_A, (i) Q_C, and (j) Q_D, respectively. Black solid line indicates the position of the bar crest.

with the MiX transport is characterized by a continuous onshore bar migration (Figure 2e), as a result of an ongoing erosion on the offshore part of the bar and the deposition in the onshore part (Figure 2f). The main drivers of the erosion-deposition pattern in the vicinity of the bar crest are the velocity and acceleration terms of the MiX transport, Q_V and Q_A (first and second terms on the RHS of equation (8)). The bottom changes of both components show a similar cross-shore pattern (Figures 2g and 2h). The bed changes driven by the divergence of the sediment transport due to currents Q_C (third term of equation (8)) are weaker (an order of magnitude lower than the Q_V and Q_A terms) and correspond to erosion in the inner face of the sandbar and accretion in the outer zone (Figure 2i). The diffusive transport term Q_D (fourth term of equation (8)) produces the flattening of the sandbar (Figure 2j). During this event the suspended-load transport components of the MiX transport are more relevant than the bed load transport terms (see supporting information). Summarizing, our third relevant finding is that velocity skewness and acceleration skewness on the sediment transport should be both accounted for.

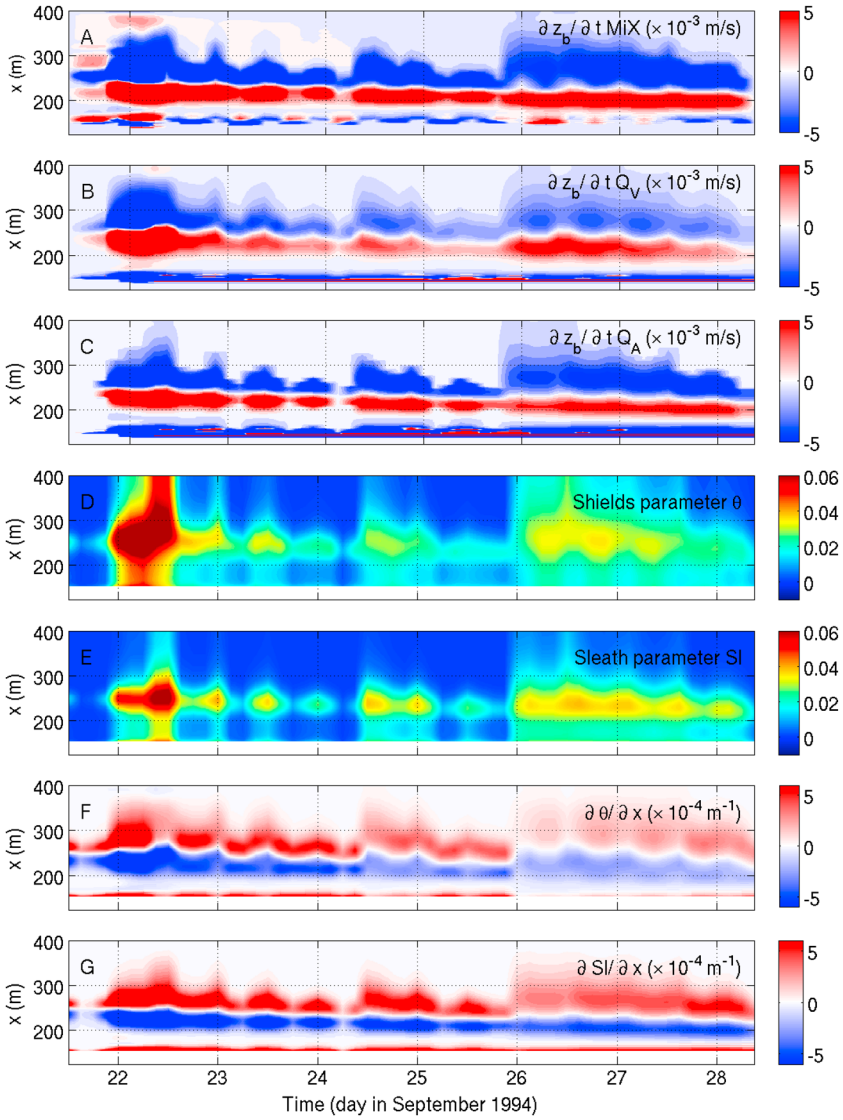

Figure 3. Time series of the bottom changes for (a) the MiX transport, (b) the Q_V term, and (c) the Q_A term. (d) Shields parameter θ' during the event; (e) Sleath parameter *Sl*; (f) spatial derivative of θ', $\partial\theta'/\partial x$; and (g) spatial derivative of the *Sl*, $\partial\theta'/\partial x$.

Our fourth important finding is that the morphodynamics of the shoaling zone is mainly driven by the velocity skewness (related to bed shear stresses), while the morphodynamics of the inner surf zone is mainly controlled by acceleration skewness (related to pressure gradients, see *Foster et al.* [2006]). This could be expected because in the shoaling zone, wave-induced velocities become skewed, as wave surface changes from a sinusoidal to a pitched-forward face shape; onshore velocities are stronger than offshore velocities, and the sediment is then driven onshore. Indeed, field experiments [*Marino-Tapia et al.*, 2007] have shown that velocity skewness is the main transport mechanism in the shoaling zone. On the other hand, as the waves approach the breaking point, usually near the bar crest, wave velocity asymmetry increases producing strong accelerations that move sediment onshore. The action of near-bed accelerations driving sediment onshore has been analyzed by *Foster et al.* [2006]. They provided field evidence that the incipient sediment motion is induced by fluid accelerations driven by pressure gradients. Besides the pressure forces, an asymmetry in bed shear stress is another physical driver of sediment transport under acceleration-skewed waves [*Calantoni and Puleo*, 2006; *Abreu et al.*, 2013]. Therefore, both velocity skewness and acceleration skewness can act together in nature and provide the physical background of the MiX transport.

To substantiate our fourth point, the wave-averaged magnitudes of the Shields parameter θ' and the Sleath parameter SI are considered. They are given by

$$\theta' = \frac{1/2\rho f_{cw}\langle|\vec{U}_t||U_{t,x}|\rangle}{(\rho_s - \rho)gd_{50}} \tag{10}$$

and

$$SI = \frac{\rho\langle(\partial|U_{t,x}|/\partial t)\rangle}{(\rho_s - \rho)gd_{50}} \tag{11}$$

where ρ is the water density, ρ_s is the sediment density, and f_{cw} is the wave and currents friction factor (set to 0.02). The Shields parameter θ' (nondimensional bed shear stress) is related to the magnitude of the near-bottom velocity and, therefore, to the SkV transport. The Sleath parameter is related to the local derivative of the near-bottom velocity and, thus, to the SkA transport. Values of the bottom changes, the θ' and SI parameters and their corresponding gradients during the event, are shown in Figure 3. During all the event, the action of bed shear stresses in the outer zone of the profile results in the bottom changes in this zone (Figures 3a, 3b, 3d, and 3f). Eventually, under the high-energy conditions during 22 September (Figure 2), pressure gradients increase in the outer zone. At low energy conditions (from 23 to 26 September), the bottom change in the offshore zone is dominated by the action of bed shear stresses. In the bar crest, both bed shear stresses and pressure gradients are present, showing the back and forth action of the pressure gradients as tides rise or fall, respectively. This is consistent with the fact that during the low tide, the bar is in the inner surf zone while during the high tide it is in the shoaling zone. Finally, the results of the last stage (moderate wave heights conditions) clearly show that SI is dominant with respect to the action of θ' in the inner surf zone (155 m $< x <$ 185 m). On the contrary, in the outer zone ($x >$ 265 m) bed shear stresses are dominant.

Since it has been demonstrated that the wave velocity and acceleration skewness play a key role on modeling the onshore sandbar migration, the modeled intrawave motion has been compared with measurements in terms of these characteristics. The comparison shows that there is a good agreement between both intrawave motions (detailed in the supporting information). Lastly, it should be noted that additional experiments, in which the acceleration $\vec{a}(t)$ is computed as the total time derivative of $\vec{U}_t$ instead of using the local time derivative, lead to similar results.

4. Conclusions

With the help of a full process-based morphodynamic model, it has been shown that accounting for the joint action of both velocity and acceleration skewnesses causes major improvement of the modeled onshore bar migration and is essential to accurately model the evolution of the entire cross-shore bottom profile. The sediment transport has a remarkable spatial dependence with regard to the wave propagation along the profile. Two regions should be distinguished: the shoaling zone, where the velocity skewness dominates the sediment transport that is mainly induced by bed shear stresses, and the breaking and inner surf zone, where the acceleration skewness dominates and sediment transport is mainly induced by pressure gradients.

Moreover, model results confirm that sediment transport based solely on either velocity skewness or acceleration skewness can achieve accurate reproduction of the onshore sandbar migration, yet they can lead to significant mismatches away from the bar zone. Therefore, results in which sediment transport was computed from the observed velocities and for which both the velocity [*Hsu et al.*, 2006] and acceleration [*Hoefel and Elgar*, 2003] skewness can cause the onshore sandbar migration are confirmed. In order to achieve good results, it is necessary to describe realistically [*Abreu et al.*, 2010; *Ruessink et al.*, 2012] the intrawave orbital motion in process-based models.

All these findings are subject to some limitations to be considered. One of the main assumptions on beach profile evolution models is the alongshore uniformity. In this sense, the alongshore variations in bathymetry induce variations in the wave properties and in the currents, affecting the cross-shore transport and originating gradients in the longshore transport, and these have been disregarded. Moreover, the results presented here are, like the previous works of *Hoefel and Elgar* [2003] and *Hsu et al.* [2006], site-specific and are focused on one short event with mostly normal wave incidence. On the other hand, on testing the

model under high-energy conditions to reproduce an offshore migration event, the model can simulate the seaward migration linked to the sandbar decay but not a pure offshore migration. Further research should validate the present findings on the effects of velocity and acceleration skewness on sediment transport for different geomorphic settings and wave conditions.

Acknowledgments

Data are provided by the Field Research Facility, Field Data Collections and Analysis Branch, US Army Corps of Engineers, Duck, North Carolina. We acknowledge funding from the Spanish research projects CTM2009-11892 and CTM2012-35398. The authors wish to thank G. Coco for his valuable comments and suggestions on the manuscript and F. Ribas for providing us the challenge to initiate this research.

The Editor thanks two anonymous reviewers for their assistance in evaluating this paper.

References

Abreu, T., P. A. Silva, F. Sancho, and A. Temperville (2010), Analytical approximate wave form for asymmetric waves, *Coastal Eng.*, *657*, 656–667.

Abreu, T., H. Michallet, P. Silva, F. Sancho, D. van der A, and B. Ruessink (2013), Bed shear stress under skewed and asymmetric oscillatory flows, *Coastal Eng.*, *73*, 1–10.

Calantoni, J., and J. A. Puleo (2006), Role of pressure gradients in sheet flow of coarse sediments under sawtooth waves, *J. Geophys. Res.*, *111*, C01010, doi:10.1029/2005JC002875.

Drake, T. G., and J. Calantoni (2001), Discrete particle model for sheet flow sediment transport in the nearshore, *J. Geophys. Res.*, *106*(C9), 19,859–19,868.

Dubarbier, B., B. Castelle, V. Marieu, and G. Ruessink (2013), Numerical modeling of pronounced sloping beach profile evolution: Comparison with the large-scale BARDEX II experiment, *J. Coastal Res.*, *65*, 1762–1767.

Elgar, S., E. L. Gallagher, and R. T. Guza (2001), Nearshore sandbar migration, *J. Geophys. Res.*, *106*(C6), 11,623–11,628.

Fernandez-Mora, A., D. Calvete, A. Falques, F. Ribas, and D. Idier (2013), On the predictability of mid-term cross-shore profile evolution, *J. Coastal Res.*, *65*, 476–481.

Foster, D. L., A. J. Bowen, R. A. Holman, and P. Natoo (2006), Field evidence of pressure gradient induced incipient motion, *J. Geophys. Res.*, *111*, C05004, doi:10.1029/2004JC002863.

Gallagher, E., S. Elgar, and R. T. Guza (1998), Observations of sand bar evolution on a natural beach, *J. Geophys. Res.*, *103*(C2), 3203–3215.

Grasso, F., H. Michallet, and E. Barthelemy (2011), Sediment transport associated with morphological beach changes forced by irregular asymmetric, skewed waves, *J. Geophys. Res.*, *116*, C03020, doi:10.1029/2010JC006550.

Henderson, S. M., J. S. Allen, and P. A. Newberger (2004), Nearshore sandbar migration predicted by an eddy-diffusive boundary layer model, *J. Geophys. Res.*, *109*, C06024, doi:10.1029/2003JC002137.

Hoefel, F., and S. Elgar (2003), Wave-induced sediment transport and sandbar migration, *Science*, *299*, 1885–1887.

Hsu, T., S. Elgar, and R. T. Guza (2006), Wave-induced sediment transport and onshore sandbar migration, *Coastal Eng.*, *53*, 817–824.

Marino-Tapia, I., P. Russell, T. O'Hare, M. Davidson, and D. Huntley (2007), Cross-shore sediment transport on natural beaches and its relation to sandbar migration patterns: 1. Field observations and derivation of a transport parameterization, *J. Geophys. Res.*, *112*, C03001, doi:10.1029/2005JC002893.

Rakha, K., R. Deigaard, and I. Broker (1997), A phase-resolving cross-shore sediment transport model for beach profile evolution, *Coastal Eng.*, *31*, 231–261.

Roelvink, J., and A. Reniers (1995), Report H2130. Lip 11D Delta Flume experiments. A data set for profile model validation, *Tech. Rep.*, Delft Hydraulics, Netherlands.

Roelvink, J. A., and M. J. F. Stive (1989), Bar-generating cross-shore flow mechanisms on a beach, *J. Geophys. Res.*, *94*(C4), 4785–4800.

Ruessink, B. G. (2005), Predictive uncertainty of a nearshore bed evolution model, *Cont. Shelf Res.*, *25*, 1053–1069.

Ruessink, B. G., G. Ramaekers, and L. C. van Rijn (2012), On the parameterization of the free-stream non-linear wave orbital motion in nearshore morphodynamic models, *Coastal Eng.*, *85*, 56–63.

Short, A. D. (1999), *Handbook of Beach and Shoreface Morphodynamics*, Wiley, Chichester, U. K.

Thornton, B., and R. T. Humiston (1996), Bar/trough generation on a natural beach, *J. Geophys. Res.*, *101*(C5), 12,097–12,110.

Van der Werf, J., H. Nomdem, J. Ribberink, D. Walstra, and W. Kranenburg (2012), Application of a new sand transport formula within the cross-shore morphodynamic model Unibest-TC, paper presented at 33rd International Conference on Coastal Engineering (ICCE), Santander, Spain.

Van Rijn, L. C. (2007a), Unified view of sediment transport by current and waves. I: Initiation of motion, bed roughness and bed-load transport, *J. Hydraul. Eng.*, *133*, 649–67.

Van Rijn, L. C. (2007b), Unified view of sediment transport by current and waves. II: Suspended transport, *J. Hydraul. Eng.*, *133*, 668–689.

Van Rijn, L. C., D. J. R. Walstra, B. Grasmeijer, J. Sutherland, S. Pan, and J. P. Sierra (2003), The predictability of cross-shore bed evolution of sandy beaches at the time scale of storms and seasons using process-based profile models, *Coastal Eng.*, *47*, 297–327.

Wright, D., J. Boon, S. Kim, and J. List (1991), Modes of cross-shore sediment transport on the shoreface of the Middle Atlantic Bight, *Mar. Geol.*, *96*, 19–51.